Identification of a novel basal body-localized epsilon-tubulin in *Leishmania*

Arunava Seth[*1], Anubhab Das[#1] and Rupak Datta[*1]

[1]Department of Biological Sciences, Indian Institute of Science Education and Research (IISER) Kolkata, Mohanpur, West Bengal, India.

*Corresponding authors:

Rupak Datta

Email: rupakdatta@iiserkol.ac.in

ORCID ID- 0000-0003-1820-9251

Arunava Seth

Email: as16ip009@iiserkol.ac.in

ORCID ID- 0000-0001-8544-3457

#Worked at the Department of Biological Sciences, IISER Kolkata as a summer intern; present address: Department of Ophthalmology, Visual and Anatomical Sciences, Wayne State University School of Medicine, Detroit, MI, USA

Running title: Epsilon tubulin of *Leishmania*

Keywords: Epsilon-tubulin, *Leishmania*, tubulin, cytoskeleton, basal body, nocodazole

Summary Statement

We report for the first time an epsilon-tubulin in *Leishmania* parasite. This nocodazole-insensitive unconventional tubulin is expressed constitutively and found to be localized in the basal body.

Abstract

Epsilon-tubulins are unconventional isoforms of the tubulin family, found in only a few organisms so far. We identified a novel epsilon-tubulin in *Leishmania major* (Lmε-tubulin) that exhibits significant sequence similarity and conservation of functional domains with its known counterparts. Lmε-tubulin was found to be constitutively expressed in both the extracellular promastigote form of the parasite and the amastigotes residing within infected macrophages. For localization studies, we generated a *Leishmania* strain expressing mNeonGreen-tagged Lmε-tubulin using CRISPR-Cas9-mediated endogenous protein tagging method. Imaging studies with this strain revealed Lmε-tubulin to be localized near the kinetoplast and at the flagellar base, indicating a basal body localization. That Lmε-tubulin is indeed localized at the basal body and not a part of the microtubular network was confirmed when its localization was found to remain unaltered upon treatment with nocodazole, a microtubule disruptor. This is the first experimental finding of an ε-tubulin not only in the genus *Leishmania* but in the entire *Trypanosomatidae* family and is likely to incite further research to uncover the physiological role of this intriguing tubulin in this group of protozoan parasites.

Introduction

Leishmania species are causal agents for leishmaniasis, a group of diseases with diverse clinical manifestations. Depending on the species involved, the symptoms of leishmaniasis can range from fatal infections of the spleen and liver to self-resolving skin lesion (Burza et al., 2018). Despite this diversity of symptoms, all *Leishmania* species share a similar digenetic life cycle involving a sandfly vector, typically from the genus *Phlebotomus* or *Lutzomyia*, and a mammalian host such as humans. During this lifecycle, the parasite switches between two distinct morphological forms. In the insect stage, it appears as a long, slender promastigote with a motile flagellum. After infecting the host macrophages, the promastigotes transform into small, rounded amastigotes with short, non-motile flagellum. This promastigote-to-amastigote transition is crucial for the survival of intracellular *Leishmania*. The drastic morphological changes involved in this process requires substantial cytoskeletal restructuring (Gluenz et al., 2010; Sunter and Gull, 2017).

Tubulins, along with actin, are pivotal in regulating cytoskeleton dynamics. They play crucial roles in various cellular functions such as vesicular trafficking, cell shape maintenance and cell cycle progression in most eukaryotic cells, including lower eukaryotes like *Leishmania* (Dandugudumula et al., 2022; Fourriere et al., 2020; Gull, 1999; Janke and Chloë Bulinski, 2011; Pollard and Cooper, 2009). Microtubule organizing centers (MTOCs) are the primary nucleation sites for tubulin polymerization. The MTOCs exist in different forms, such as basal bodies associated with cilia or flagella, and centrosomes linked to mitotic spindles (Wu and Akhmanova, 2017). In *Leishmania* as well as in other members of the *Trypanosomatidae* family, the basal body is closely associated with the kinetoplast near the flagellar pocket, a site through which processes like endocytosis or exocytosis occur (Field and Carrington, 2009; Overath et al., 1997; Sengupta et al., 1999; Stierhof et al., 1994). It also plays critical role in

formation and anchoring of the flagellum thereby acting as controlling center for parasite's motility, attachment and infectivity (Halliday et al., 2020; Sunter et al., 2019).

The *Leishmania* basal body is reported to form axoneme structure of classical 9+2 arrangement of microtubules in the promastigote form and a 9+0 arrangement in the amastigotes (Alexander, 1978; Rudzinska et al., 1964; Wheeler et al., 2015). Limited investigations on the *Leishmania* basal body composition have so far identified only a few key proteins, such as centrin, centrin4, protein of centriole, and SAS6 (Selvapandiyan et al., 2001; van Breugel et al., 2014; Vats et al., 2023). Apart from these, γ-tubulin is also known to localize in its basal body (Libusová et al., 2004). In contrast, alpha and beta-tubulin of *Leishmania* act as monomers for protofilaments forming microtubules but are not part of the basal body (Fong and Lee, 1988; Wirth and Slater, 1983). However, the presence of other unconventional tubulin isoforms, such as epsilon, delta, and zeta tubulins, remains to be experimentally validated in *Leishmania* as well as in other parasites of the *Trypanosomatidae* family.

The epsilon, delta, and zeta-tubulins, collectively grouped as evolutionary co-conserved ZED module, are predicted to be present in most eukaryotes, ranging from unicellular protists to higher-order mammals (Turk et al., 2015). Interestingly, genome analysis across various organisms revealed a unique pattern of conservation of the ZED module tubulins. It was observed that organisms lacking epsilon-tubulin were also missing delta and zeta-tubulins, while those possessing epsilon-tubulin consistently had delta and/or zeta-tubulin as well. This observation suggests that epsilon-tubulin might be playing a central role in coordinating the function of ZED module, acting in partnership with delta and/or zeta-tubulin (Turk et al., 2015). Epsilon-tubulin was first predicted in *Saccharomyces cerevisiae* by RG Burns through extensive bioinformatic analysis (Burns, 1995). Subsequently, it was discovered in many other organisms, including humans (Chang and Stearns, 2000; Dupuis-Williams et al., 2002; Dutcher et al., 2002; Ross et al., 2013). In human cells, the epsilon-tubulin was found to localize in the

centrosome but at a distinct site from γ-tubulin (Chang and Stearns, 2000). Recently, it has been shown that knocking out epsilon-tubulin in human hTERT RPE-1 cells results in the formation of abnormal centrioles lacking triplet microtubules (Wang et al., 2017). Epsilon-tubulin from *Xenopus laevis*, which is similar to its human counterpart in terms of sequence and localization, has been reported to be important for centriole duplication (Chang et al., 2003). In mice, epsilon-tubulin has been shown to be crucial for forming complex microtubule arrays, and its absence resulted in drastic loss of germ cells leading to male sterility (Stathatos et al., 2024). The basal body-localized epsilon-tubulin of *Paramecium* was found to play essential role in the assembly and anchorage of the centriolar microtubules (Dupuis-Williams et al., 2002). In *Tetrahymena thermophila*, deletion or mutation of the epsilon-tubulin gene caused flagellar defects, with some mutations proving to be lethal (Ross et al., 2013). Similarly, in *Chlamydomonas*, deletion of epsilon-tubulin resulted in failure in basal body assembly, preventing proper flagella formation (Dutcher et al., 2002). Despite these studies proving the essentiality of epsilon-tubulin in various organisms across different branches of life, its presence in the *Trypanosomatidae* group of protozoan parasites remains ambiguous. Although Vaughan *et. al.* have bioinformatically predicted the presence of epsilon-tubulin in *Trypanosoma brucei*, its experimental validation is still awaited (Vaughan et al., 2000). Recently, by employing a CRISPR-Cas9 based high-throughput endogenous protein tagging technique, Billington *et. al.* were successful in fluorescent-labeling of 89% of the *T. brucei* proteome and in mapping their subcellular localization. However, for the epsilon-tubulin, no signal above the background fluorescence was detected in their studies (Billington et al., 2023). A similar high-throughput study is underway to endogenously label the *Leishmania* proteome (Aellig et al., 2024). But till date, there is no report on epsilon-tubulin in any of the *Leishmania* species.

115 We report here identification of an epsilon-tubulin in *Leishmania major* (*L. major*), which
116 exhibited constitutive expression in both the extracellular promastigote and intracellular
117 amastigote forms of the parasite. Using CRISPR-Cas9 mediated endogenous protein tagging,
118 coupled with imaging studies, we demonstrated that this nocodazole-insensitive
119 unconventional tubulin is localized at the basal body. This is the first experimentally validated
120 epsilon tubulin in the entire *Trypanosomatidae* family. This discovery is likely to encourage
121 further structure-function studies aimed at understanding the role of epsilon tubulin in parasite
122 physiology.

123 **Results and Discussion**

124 **Identification of *L. major* epsilon-tubulin**

125 Genome sequence of *L. major* predicted the presence of a putative epsilon-tubulin on
126 chromosome 21, annotated as LmjF.21.1010 (Ivens, 2005). The predicted protein sequence of
127 *L. major* epsilon-tubulin (Lmε-tubulin) was aligned with bona fide, well-characterized epsilon-
128 tubulins from *Tetrahymena thermophila* (Ross et al., 2013), *Chlamydomonas reinhardtii*
129 (Dutcher et al., 2002), *Homo sapiens* (Chang and Stearns, 2000) and *Paramecium tetraurelia*
130 (Dupuis-Williams et al., 2002) (Fig 1). Lmε-tubulin was found to share ~ 40% sequence
131 identities and ~ 60% sequence similarities with its counterparts in these species (Fig 1, Table
132 S1). InterPro analysis confirmed the presence of signature tubulin domains, the GTPase domain
133 and C-terminal domain, in Lmε-tubulin (Fig 1; yellow and green shaded regions) (Nogales et
134 al., 1998a; Nogales et al., 1998b; Paysan-Lafosse et al., 2023). Importantly, 23 out of 27 GTP-
135 binding residues of *Tetrahymena* epsilon-tubulin are either conserved or replaced with similar
136 residues in Lmε-tubulin (Fig 1; black triangles). Also, nine out of ten amino acids, mutations
137 of which in *Tetrahymena* epsilon-tubulin led to lethal or slow-growing phenotypes, were found
138 to be conserved in Lmε-tubulin (Fig 1; black boxes) (Ross et al., 2013). Studies with
139 *Paramecium* and human epsilon-tubulins revealed that they have unique amino acid insertions,

140 which are absent in canonical tubulins (Dupuis-Williams et al., 2002; Inclán and Nogales,
141 2001). These insertions were hypothesized to be required for longitudinal contact with other
142 tubulins (Inclán and Nogales, 2001). We probed for the presence of such insertions in Lmε-
143 tubulin by aligning its sequence with α, β and γ-tubulins of *L. major* (Fig S1A). Most of the
144 regions aligned except two prominent stretches of amino acids; Insertion I (R211 - T236) and
145 Insertion II (H325 - T332) (Fig S1A). Comparison of the AlphaFold structure of Lmε-tubulin
146 with that of the structures of α, β and γ-tubulins of *L. major* showed mostly aligned regions,
147 except for the insertions I and II (Fig S1B). The sequence and structural alignment results thus
148 confirmed the presence of these characteristic insertions in Lmε-tubulin. Interestingly, we
149 observed that the C-terminal of the Lmε-tubulin also did not align properly with the α, β or γ-
150 tubulins (Fig S1B). The C-terminal residues of canonical tubulins are reported to be crucial for
151 post-translational modifications (Janke and Chloë Bulinski, 2011). So, a lack of proper
152 alignment and absence of secondary structure of Lmε-tubulin C-terminal region suggests that
153 the post-translational modifications are either absent or different from the classical tubulins. A
154 similar feature was earlier observed in the C-terminal domain of *Tetrahymena* epsilon-tubulin
155 (Ross et al., 2013). Isoforms of Lmε-tubulin were also predicted in the genomes of other
156 *Leishmania* species, each displaying very high sequence identity (>97% for *L. donovani*, *L.*
157 *infantum*, *L. mexicana* and >90% for *L. braziliensis)* (Table S1). Lmε-tubulin was found to
158 exhibit >65% sequence identity and >80% sequence similarity with putative epsilon tubulins
159 of other members of the *Trypanosomatidae* family, *T. brucei* and *T. cruzi* (Table S1).
160 Collectively, these findings from our bioinformatic analyses strongly affirm the legitimacy of
161 Lmε-tubulin as an authentic epsilon tubulin.

162 **Promastigote and amastigote forms of *L. major* both expresses epsilon-tubulin**

163 Analysis of the genetic locus revealed that the *Lmε-tubulin* is flanked upstream by a
164 hypothetical gene (LmjF.21.1000) and downstream by the putative dynein arm light chain

165 encoding gene (LmjF.21.1020) (Fig 2A). To experimentally verify the presence of *Lmε-tubulin*
166 in the genome, we used *L. major* genomic DNA as the template for PCR amplification of the
167 corresponding segment using *Lmε-tubulin*-specific primers (P1 & P2). A 1413 bp product was
168 obtained, which matched with the expected size of *Lmε-tubulin* coding region (Fig 2B). After
169 confirming the presence of *Lmε-tubulin* in the genome, our next goal was to check its
170 expression. For this, cDNAs, prepared from *L. major* promastigote mRNAs, were subjected to
171 PCR amplification with primers, P1 & P2. This RT-PCR yielded 1413 bp product, confirming
172 the expression of Lmε-tubulin mRNA in the promastigote stage (Fig 2C). Since many genes of
173 *Leishmania* exhibit stage-specific expression pattern, we wanted to verify whether Lmε-tubulin
174 is expressed in the intracellular amastigote form also (Brotherton et al., 2010). For this, as
175 described schematically in Fig 2D, we infected J774A.1 macrophage cells with *L. major*
176 promastigotes and isolated total mRNAs from the infected macrophages at ~ 60 hours post-
177 infection (to allow promastigote-to-amastigote transformation). This pool of mRNA was a
178 mixture derived from both host macrophage cells and the intracellular amastigotes. When RT-
179 PCR was performed with primers P1 & P2 using this mRNA pool from the *Leishmania* infected
180 macrophages, a 1413 bp product got amplified confirming the presence of Lmε-tubulin
181 transcripts in the amastigotes. That this product was not a non-specific amplification from
182 macrophage mRNA was confirmed when we found that mRNA isolated from uninfected
183 macrophages did not yield any product upon RT-PCR (Fig 2E).

184 **CRISPR-Cas9 mediated tagging of endogenous epsilon-tubulin with mNeonGreen**

185 Determining the localization of a protein is a prerequisite to understand its function. To
186 examine the localization of Lmε-tubulin, we planned to tag the endogenous protein with the
187 fluorophore mNeonGreen using CRISPR-Cas9 gene editing technology (Beneke et al., 2017).
188 For this, we first generated an *L. major* strain expressing *Streptococcus pyogenes* Cas9
189 (SpCas9) and T7 Polymerase (T7Pol). The strain was verified using genomic DNA PCR, using

190 primers specific for SpCas9 and T7pol. This produced 4.1 kb and 2.7 kb PCR products,
191 respectively, confirming successful integration of SpCas9 and T7pol in the *L. major* genome
192 (Fig S2). This strain, referred to as LmCas9:T7Pol, was used to generate the N-terminal
193 mNeonGreen (mNG)-tagged-Lmε-tubulin expressing *L. major* (Fig 3A), as described in details
194 in the materials and methods section and in Fig S3. When the whole cell lysate of this
195 engineered strain was subjected to western blot with anti-mNG antibody, an 82.8 kDa band
196 corresponding to the molecular weight of the fusion protein (31.1 kDa: 3XMyc-mNeonGreen,
197 and 51.7 kDa: Lmε-tubulin) was observed. As expected, no band was observed when similar
198 western blot was performed with the lysates from control cells (wild type *L. major* or
199 LmCas9:T7Pol) (Fig 3B).

200 **The epsilon-tubulin is localized at two distinct spots in the basal body of *L. major***

201 After successful validation of the (mNG)-tagged-Lmε-tubulin expression *L. major* strain, we
202 aimed to determine intracellular localization of Lmε-tubulin in both promastigotes and
203 intracellular amastigotes. Confocal microscopy of the (mNG)-tagged-Lmε-tubulin expressing
204 *L. major* promastigotes revealed two bright fluorescent spots in the cell body, one in close
205 association with the kinetoplast DNA and the other at the base of the flagella (Fig 3C). Such a
206 distinct pattern of fluorescent signal indicates basal body localization of Lmε-tubulin. The
207 localization pattern of Lmε-tubulin is reminiscent of centrin, another basal body-localized
208 protein of the parasite (Selvapandiyan et al., 2001). To check the localization of Lmε-tubulin
209 in the intracellular amastigote stage, confocal images were acquired directly from the J774A.1
210 macrophages infected with the (mNG)-tagged-Lmε-tubulin expressing *L. major* strain. Such
211 direct image acquisition method ensures authenticity of the amastigote-character of the
212 parasite, which could otherwise be altered if amastigotes were isolated from the infected
213 macrophages prior to imaging. Like in promastigotes, two distinct fluorescent spots in close

214 proximity of the kinetoplast and the flagellar base were observed in the amastigotes as well
215 (Fig 3D).
216 To validate basal body localization Lmε-tubulin, we treated the (mNG)-tagged-Lmε-tubulin
217 expressing *L. major* promastigotes with nocodazole, a known microtubule depolymerizer that
218 does not disrupt the basal body structure. Previous studies in U2OS cells have demonstrated
219 that nocodazole treatment does not affect the localization of human epsilon and delta tubulins,
220 as they are associated with the centrosome and are not part of the microtubular network (Chang
221 and Stearns, 2000; Debrabander et al., 1977). We observed that the localization of Lmε-tubulin
222 indeed remained unchanged in >90% of the cells upon treatment with 1 μM nocodazole (Fig
223 4A, B). To rule out the possibility that nocodazole does not work on *Leishmania* cells, we
224 decided to perform a control experiment to verify if nocodazole treatment could disrupt the
225 localization of α-tubulin, which is an integral part of the microtubular network (McKenna et
226 al., 2023). For this, we generated a mNG- α-tubulin *L. major* strain following similar CRISPR-
227 Cas9-based gene editing method. The authenticity of the strain was confirmed by western blot
228 with anti-mNG antibody, showing a 80.8 kDa band corresponding to the fusion protein (Fig
229 S4). The untreated mNG-α-tubulin in *L. major* promastigotes exhibited characteristic
230 microtubule localization pattern, predominantly along the periphery of the cell, as previously
231 reported earlier in *L. mexicana* (Tran et al., 2015). When these cells were treated with
232 nocodazole, it was observed that unlike the Lmε-tubulin, which was largely insensitive to the
233 drug, the α-tubulin localization pattern drastically changed due to microtubule disassembly
234 (Fig 4C, D). Taken together, these data provided unambiguous evidence that Lmε-tubulin is
235 indeed localized at the basal body and not part of the broader microtubular network. In this
236 context it is worth mentioning that epsilon tubulin isoforms from *Tetrahymena*,
237 *Chlamydomonas*, *Paramecium* and human have been also shown to localize in the basal body
238 (Chang and Stearns, 2000; Dupuis-Williams et al., 2002; Dutcher et al., 2002; Ross et al.,

239 2013). This suggests that Lmε-tubulin may share functional similarity with its counterparts in
240 these organisms.
241 In conclusion, we identified for the first time a constitutively expressed, basal body-localized
242 ε-tubulin not only in the genus *Leishmania* but in the entire *Trypanosomatidae* family.
243 However, further studies, including genetic knockout of Lmε-tubulin, are necessary to
244 definitively establish the role of this unconventional tubulin in basal body stability and
245 maintenance. It will be also important to investigate Lmε-tubulin's interaction of with other
246 tubulin isoforms to gain a comprehensive understanding of the microtubule dynamics,
247 especially during promastigote-to-amastigote transition. In particular, investigating the status
248 of ZED module partners of Lmε-tubulin, such as delta and zeta-tubulin, would be very
249 interesting to provide deeper insights into the complex interactions that govern the basal body
250 dynamics in *Leishmania* and other trypanosomatid parasites. The CRISPR-Cas9 mediated
251 endogenous protein tagging method employed here to label Lmε-tubulin can prove to be very
252 useful for detailed study of the basal body architecture and in identifying different proteins
253 associated with it. Our work is likely to stimulate further research towards these directions.

254 **Material and Methods**

255 All reagents were purchased from Sigma-Aldrich unless otherwise mentioned. Primers used
256 for PCR were obtained from Integrated DNA Technologies and their sequence information are
257 provided in Table S2. Details of antibodies used in this study are mentioned in Table S3.

258 ***Leishmania* and mammalian cell culture**

259 *L. major* strain (MHOM/SU/73/5-ASKH) and J774A.1 murine macrophages were procured
260 from ATCC. *L. major* promastigotes were cultured as described before (Pal et al., 2015).
261 Briefly, *L. major* cells were grown at 26 ^{0}C in M199 medium (Gibco) supplemented with 15%
262 heat-inactivated fetal bovine serum (Gibco), 23.5 mM HEPES, 0.2 mM adenine, 150 µg/ml
263 folic acid, 10 µg/ml hemin, 120 U/ml penicillin, 120 µg/ml streptomycin, and 60 µg/ml

264 gentamicin. J774A.1 murine macrophages were cultured in Dulbecco's modified Eagle's
265 medium (Gibco) pH 7.4, supplemented with 10% heat-inactivated fetal bovine serum, 2 mM
266 L-glutamine, 100 µg/ml streptomycin and 100 U/ml penicillin at 37 °C in a humidified
267 atmosphere containing 5% CO_2. Whenever necessary, a hemocytometer was used to count cells
268 fixed with 0.9% formal saline or stained with Trypan blue.

269 **Sequence alignment and bioinformatics**

270 Sequence alignment was performed using the Clustal Omega
271 (https://www.ebi.ac.uk/jdispatcher/msa/clustalo). NCBI Blast (https://blast.ncbi.nlm.nih.gov/
272 Blast.cgi) was used to determine the percent identity and similarity. The result was copied and
273 modified for presentation using MS Word processor and Inkscape without changing any base
274 value. Mutated residues were manually colored as per the literature (Ross et al., 2013) and the
275 tubulin mutation database (https://tubulinmutations.bio.uci.edu/.html). Domains were
276 predicted based on InterPro analysis (https://www.ebi.ac.uk/interpro/). The following protein
277 sequences were obtained from UniProt, epsilon-tubulins from *L. major* (Q4QC95), *T.*
278 *thermophila* (Q22YZ9), *C. reinhardtii* (A0A2K3DX56), *Homo sapiens* (Q9UJT0),
279 *Paramecium tetraurelia* (Q8WPW7), *L. donovani (A0A3Q8IAD6), L. mexicana* (E9AV85)*, L.*
280 *braziliensis* (A4HBW1)*, L. infantum* (E9AGW9)*, T. cruzi* (A0A7J6XYD9)*, T. brucei*
281 (Q9NI44) *L. major* α-tubulin (Q4QGC5), *L. major* β-tubulin (Q4Q4C4), *L. major* γ-tubulin
282 (Q4Q9Z8). The predicted structure for *L. major* α-, β- and γ-tubulin was obtained from the
283 AlphaFold server (Jumper et al., 2021; Varadi et al., 2022). Structural alignment was done using
284 the ChimeraX software module (Pettersen et al., 2004).

285 **Genomic DNA PCR**

286 The genomic DNA of *L. major* promastigotes was isolated using the phenol-chloroform
287 method. Briefly, 1 x10^7 *L. major* cells were harvested and resuspended in 0.1 ml lysis buffer
288 (0.1 M Tris-Cl, 0.1 M NaCl, 1% SDS, 100 mM EDTA, 100 µg/ml Proteinase K) and incubated

289 at 55 ^{0}C for 120 minutes. 25 µl phenol and 25 µl chloroform were added to the lysate and
290 centrifuged at 13000g for 15 minutes. The upper aqueous phase was taken in a fresh tube, and
291 an equal volume of chloroform was added and centrifuged at 13000g for 15 minutes. The
292 supernatant was collected, and 1/10 volume 3 M sodium acetate and 2 volume ethanol were
293 added and centrifuged at 13000g for 10 minutes. The pellet is washed with 70% ethanol twice
294 and eluted in nuclease-free water. DNA Concentration was determined spectrophotometrically
295 using NanoDrop spectrophotometer. Genomic DNA PCR amplification was performed using
296 Leo Mastermix (Dxbidt, India) and specific primers following manufacturer's protocol.

297 **Checking of Lmε-tubulin expression in *L. major* promastigote**

298 Total RNA from *L. major* promastigotes was isolated using Trizol reagent (Invitrogen)
299 followed by DNase I treatment (Invitrogen). cDNA was prepared from DNase I-treated RNA
300 using Verso cDNA kit (Thermo Scientific) using the manufacturer's protocol. -RT controls
301 were prepared from DNase I treated RNA where all Verso cDNA kit components were added
302 except the reverse transcriptase enzyme. PCR was performed using the cDNAs from +RT and
303 -RT samples.

304 **Checking of Lmε-tubulin expression in *L. major* amastigote**

305 *L. major* infection of J774A.1 macrophages was performed as described by us before (Pal et
306 al., 2017). Briefly, J77A.1 macrophages were activated in the presence of 100 ng/ml LPS for 6
307 hours, and to it stationary phase *L. major* cells were added at MOI 1:30. After 12 hours, media
308 was discarded to remove uninternalized parasites, and washed with 1X PBS, and fresh DMEM
309 media was added, and incubated for ~60 hours. Total RNA was extracted from infected and
310 uninfected macrophages and RT-PCR was performed following the protocol described above.

311 **LmCas9:T7Pol *L. major* strain generation**

312 LmCas9:T7Pol expressing *L. major* cells were generated following protocols and plasmid
313 developed by Beneke et al. (Beneke et al., 2017) with slight modification. pTB007 cells were

314 electroporated into wild-type *L. major* cells. 30 µg of the plasmid was resuspended in an
315 electroporation buffer (21 mM HEPES, 0.7 mM NaH_2PO_4, 137 mM NaCl, and 6 mM glucose;
316 pH 7.4) and electroporated using BTX Gemini electroporator (480 V, 550 µF, 25 ohms) to 4
317 x10^7 *L. major* promastigotes. The cells were selected in the presence of 50 µg/ml Hygromycin.
318 Total genomic DNA was isolated from selected cells and subjected to PCR to verify the
319 generated strain. The PCR was conducted with P3/P4, P5/P6 and P7/P8 for amplification of
320 SpCas9, T7pol and rRNA45, respectively.

321 **Generation of N-terminal mNG-tagged-epsilon/alpha-tubulin expressing *L. major* strains**

322 The N-terminal mNG-tagged-epsilon/alpha-tubulin expressing *L. major* strains were generated
323 following the protocol reported by Beneke et al. (Beneke et al., 2017) and as schematically
324 described in Fig S3. The primers used for the strain generation were designed using the
325 LeishGEdit primer design module (http://www.leishgedit.net/Home.html) and the primer
326 sequences are provided in Table S2. For preparation of sgDNA (template for sgRNA), overlap
327 extension PCR was performed using primer P11 (for ε-tubulin) or P14 (for α-tubulin) and
328 primer G00 (containing sgRNA scaffold sequence). Donor DNA containing blasticidin resistant
329 gene flanked by 30 nucleotide upstream and downstream sequence of the Cas9-cleavage site
330 was PCR amplified using pPLOTv1 blast-mNG-blast plasmid as template and primers P9/P10
331 (for ε-tubulin) and P12/P13 (for α-tubulin). All the PCR amplifications were done using PFU
332 polymerase following the protocol mentioned by Beneke et al., 2017 (Beneke et al., 2017). The
333 donor DNAs were gel eluted using commercial kit (BioBharati). The eluted donor DNA and
334 corresponding sgDNA were simultaneously electroporated into LmCas9:T7Pol *L. major* cells
335 and selected in 20 µg/ml blasticidin S containing media for ~7 days.

336 **Western blotting**

337 Whole cell lysate was prepared in 1X resuspension buffer (1X PBS+1X protease inhibitor
338 cocktail) with sonication. Protein amount was quantified using Lowry method and 40 µg of

339 whole cell lysate were loaded in 12% polyacrylamide gel and subjected to SDS-PAGE. The
340 protein was transferred to PVDF membrane and blocked with blocking solution (5% skim milk
341 solution in TBST (10 mM Tris, 150 mM NaCl, 0.025% Tween 20)). The membrane is washed
342 for 5 minutes for two times and incubated overnight with shaking at cold room with rabbit anti-
343 mNG primary antibody and rabbit anti-LdActin diluted in TBST (Table S3). The membrane
344 was washed with 1X TBST for 5 minutes 5 times and incubated with HRP tagged goat anti-
345 rabbit secondary antibody for 1.5 hours in room temperature. The membrane was washed with
346 1X TBST for 5 minutes for 5 times. Using chemiluminescent substrate (Biorad), blot was
347 developed and signal documented in ChemiDoc imaging system (Biorad).

348 **Imaging studies**

349 mNG-ε-tubulin expressing *L. major* promastigotes were spread on poly-L-lysine-coated
350 coverslips and incubated for 30 minutes. Fixation solution (4% paraformaldehyde in 1X PBS)
351 was added to it and incubated in dark for 10 mins. The coverslips were washed twice with 1X
352 PBS and mounted in antifade mounting media with DAPI (Vectashield). The images were
353 acquired in Leica SP8 confocal microscope using a 63X oil immersion lens. Images were
354 processed using LasX (Leica). Central 1-3 stacks were merged and projected for representation.
355 mNG-ε-tubulin expressing *L. major* amastigote inside macrophages were imaged by the same
356 protocol with slight modification. J774A.1 macrophages were infected with mNG-tagged-ε-
357 tubulin *L. major* cells as described above. At ~60 hours post infection, macrophages were fixed,
358 washed twice with 1X PBS and mounted in antifade mounting media with DAPI (Vectashield).
359 The images were acquired in Leica SP8 confocal microscope using a 63X oil immersion lens.
360 Images were processed using LasX (Leica). Central 1-3 stacks were merged and projected for
361 representation.

362 **Nocodazole disruption assay**

363 mNG-tagged-epsilon/alpha-tubulin expressing *L. major* promastigotes ($1x10^7$ cells) were
364 incubated with 1 μM Nocodazole or DMSO (as control) in 200 μl M199 media for 1 hour. Cells
365 were spread on a poly-L-lysine coated coverslip and fixed with 4% paraformaldehyde for 10
366 minutes. Coverslips were washed twice with 1X PBS, mounted in antifade mounting media
367 with DAPI (Vectashield) and imaged immediately in Leica SP8 confocal microscope.
368 Individual stacks were analyzed and represented. The percentage of cells with unaltered
369 localization of the respective tubulins (ε or α) were calculated for both untreated and
370 nocodazole treated cells. In the case of α-tubulin, the cytoskeleton is considered intact if the
371 peripheral tubulin signal is clearly visible. In the case of ε-tubulin strain, if two distinct puncta
372 are visible, it is considered as unaltered.

373 **Acknowledgment**

374 The authors thank Dr. Sankar Maiti and Dr. Subhra Majumder for sharing reagents and for
375 providing valuable suggestions. Dr. Subrata Adak and Dr. Amogh Sahasrabuddhe are
376 acknowledged for providing the plasmids for CRISPR-Cas9 manipulation and LdActin
377 antibody, respectively. Dr. Subhankar Dolai is thanked for his critical comments on the
378 manuscript.

379 **Funding**

380 This work was supported by Indian Council of Medical Research (ICMR) research grant No:
381 6/9-7(318)/2023-ECD-II and West Bengal DSTBT grant No: 398(Sanc.)/STBT-
382 13015/16/2024-ST SEC awarded to RD. AS was supported by CSIR NET fellowship.

383 **Competing interests**

384 No competing interests declared

385 **Data and resource availability**

386 All other data that supports the results of this study are available from the corresponding author
387 (rupakdatta@iiserkol.ac.in) upon reasonable request.

References

Aellig, S., Billington, K., Damasceno, J. D., Davidson, L., Dobramysl, U., Etzensperger, R., Ferreira, E. R., Gluenz, E., Mottram, J. C., Neish, R., et al. (2024). LeishGEM: genome-wide deletion mutant fitness and protein localisations in Leishmania. *Trends in Parasitology* 40, 675–678.

Alexander, J. (1978). Unusual axonemal doublet arrangements in the flagellum of Leishmania amastigotes. *Transactions of the Royal Society of Tropical Medicine and Hygiene* 72, 345–347.

Beneke, T., Madden, R., Makin, L., Valli, J., Sunter, J. and Gluenz, E. (2017). A CRISPR Cas9 high-throughput genome editing toolkit for kinetoplastids. *R. Soc. open sci.* 4, 170095.

Billington, K., Halliday, C., Madden, R., Dyer, P., Barker, A. R., Moreira-Leite, F. F., Carrington, M., Vaughan, S., Hertz-Fowler, C., Dean, S., et al. (2023). Genome-wide subcellular protein map for the flagellate parasite Trypanosoma brucei. *Nat Microbiol* 8, 533–547.

Brotherton, M.-C., Racine, G., Foucher, A. L., Drummelsmith, J., Papadopoulou, B. and Ouellette, M. (2010). Analysis of Stage-Specific Expression of Basic Proteins in *Leishmania infantum*. *J. Proteome Res.* 9, 3842–3853.

Burns, R. G. (1995). Identification of two new members of the tubulin family. *Cell Motil. Cytoskeleton* 31, 255–258.

Burza, S., Croft, S. L. and Boelaert, M. (2018). Leishmaniasis. *The Lancet* 392, 951–970.

Chang, P. and Stearns, T. (2000). δ-Tubulin and ε-tubulin: two new human centrosomal tubulins reveal new aspects of centrosome structure and function. *Nat Cell Biol* 2, 30–35.

Chang, P., Giddings, T. H., Winey, M. and Stearns, T. (2003). ε-Tubulin is required for centriole duplication and microtubule organization. *Nat Cell Biol* 5, 71–76.

Dandugudumula, R., Fischer-Weinberger, R. and Zilberstein, D. (2022). Morphogenesis Dynamics in Leishmania Differentiation. *Pathogens* 11, 952.

Debrabander, M., Demey, J., Joniau, M. and Geuens, G. (1977). Ultrastructural immunocytochemical distribution of tubulin in cultured cells treated with microtubule inhibitors. *Cell Biology International Reports* 1, 177–183.

Dupuis-Williams, P., Fleury-Aubusson, A., De Loubresse, N. G., Geoffroy, H., Vayssié, L., Galvani, A., Espigat, A. and Rossier, J. (2002). Functional role of ε-tubulin in the assembly of the centriolar microtubule scaffold. *The Journal of Cell Biology* 158, 1183–1193.

Dutcher, S. K., Morrissette, N. S., Preble, A. M., Rackley, C. and Stanga, J. (2002). ε-Tubulin Is an Essential Component of the Centriole. *MBoC* 13, 3859–3869.

Field, M. C. and Carrington, M. (2009). The trypanosome flagellar pocket. *Nat Rev Microbiol* 7, 775–786.

Fong, D. and Lee, B. (1988). Beta tubulin gene of the parasitic protozoan *Leishmania mexicana*. *Molecular and Biochemical Parasitology* 31, 97–106.

Fourriere, L., Jimenez, A. J., Perez, F. and Boncompain, G. (2020). The role of microtubules in secretory protein transport. *Journal of Cell Science* 133, jcs237016.

Gluenz, E., Ginger, M. L. and McKean, P. G. (2010). Flagellum assembly and function during the Leishmania life cycle. *Current Opinion in Microbiology* 13, 473–479.

Gull, K. (1999). The Cytoskeleton of Trypanosomatid Parasites. *Annu. Rev. Microbiol.* 53, 629–655.

Halliday, C., Yanase, R., Catta-Preta, C. M. C., Moreira-Leite, F., Myskova, J., Pruzinova, K., Volf, P., Mottram, J. C. and Sunter, J. D. (2020). Role for the flagellum attachment zone in Leishmania anterior cell tip morphogenesis. *PLoS Pathog* 16, e1008494.

Inclán, Y. F. and Nogales, E. (2001). Structural models for the self-assembly and microtubule interactions of γ-, δ- and ε-tubulin. *Journal of Cell Science* 114, 413–422.

Ivens, A. C. (2005). The Genome of the Kinetoplastid Parasite, Leishmania major. *Science* 309, 436–442.

Janke, C. and Chloë Bulinski, J. (2011). Post-translational regulation of the microtubule cytoskeleton: mechanisms and functions. *Nat Rev Mol Cell Biol* 12, 773–786.

Jumper, J., Evans, R., Pritzel, A., Green, T., Figurnov, M., Ronneberger, O., Tunyasuvunakool, K., Bates, R., Žídek, A., Potapenko, A., et al. (2021). Highly accurate protein structure prediction with AlphaFold. *Nature* 596, 583–589.

Libusová, L., Sulimenko, T., Sulimenko, V., Hozák, P. and Dráber, P. (2004). γ-Tubulin in Leishmania: cell cycle-dependent changes in subcellular localization and heterogeneity of its isoforms. *Experimental Cell Research* 295, 375–386.

McKenna, E. D., Sarbanes, S. L., Cummings, S. W. and Roll-Mecak, A. (2023). The Tubulin Code, from Molecules to Health and Disease. *Annu. Rev. Cell Dev. Biol.* 39, 331–361.

Nogales, E., Wolf, S. G. and Downing, K. H. (1998a). Structure of the alpha beta tubulin dimer by electron crystallography. *Nature* 391, 199–203.

Nogales, E., Downing, K. H., Amos, L. A. and L❓we, J. (1998b). Tubulin and FtsZ form a distinct family of GTPases. *Nat Struct Mol Biol* 5, 451–458.

456 Overath, P., Stierhof, Y.-D. and Wiese, M. (1997). Endocytosis and secretion in
457 trypanosomatid parasites — Tumultuous traffic in a pocket. *Trends in Cell Biology* 7,
458 27–33.

459 Pal, D. S., Mondal, D. K. and Datta, R. (2015). Identification of Metal Dithiocarbamates as a
460 Novel Class of Antileishmanial Agents. *Antimicrobial Agents and Chemotherapy* 59,
461 2144–2152.

462 Pal, D. S., Abbasi, M., Mondal, D. K., Varghese, B. A., Paul, R., Singh, S. and Datta, R. (2017).
463 Interplay between a cytosolic and a cell surface carbonic anhydrase in pH
464 homeostasis and acid tolerance of *Leishmania*. *Journal of Cell Science* 130, 754–766.

465 Paysan-Lafosse, T., Blum, M., Chuguransky, S., Grego, T., Pinto, B. L., Salazar, G. A., Bileschi,
466 M. L., Bork, P., Bridge, A., Colwell, L., et al. (2023). InterPro in 2022. *Nucleic Acids*
467 *Research* 51, D418–D427.

468 Pettersen, E. F., Goddard, T. D., Huang, C. C., Couch, G. S., Greenblatt, D. M., Meng, E. C. and
469 Ferrin, T. E. (2004). UCSF Chimera—A visualization system for exploratory research
470 and analysis. *J Comput Chem* 25, 1605–1612.

471 Pollard, T. D. and Cooper, J. A. (2009). Actin, a Central Player in Cell Shape and Movement.
472 *Science* 326, 1208–1212.

473 Ross, I., Clarissa, C., Giddings, T. H. and Winey, M. (2013). ε-tubulin is essential in
474 *Tetrahymena thermophila* for the assembly and stability of basal bodies. *Journal of*
475 *Cell Science* jcs.128694.

476 Rudzinska, M. A., D'Alesandro, P. A. and Trager, W. (1964). The Fine Structure of *Leishmania*
477 *donovani* and the Role of the Kinetoplast in the Leishmania-Leptomonad
478 Transformation*. *The Journal of Protozoology* 11, 166–191.

479 Selvapandiyan, A., Duncan, R., Debrabant, A., Bertholet, S., Sreenivas, G., Negi, N. S., Salotra,
480 P. and Nakhasi, H. L. (2001). Expression of a Mutant Form of Leishmania donovani
481 Centrin Reduces the Growth of the Parasite. *Journal of Biological Chemistry* 276,
482 43253–43261.

483 Sengupta, S., Tripathi, J., Tandon, R., Raje, M., Roy, R. P., Basu, S. K. and Mukhopadhyay, A.
484 (1999). Hemoglobin Endocytosis in Leishmania Is Mediated through a 46-kDa Protein
485 Located in the Flagellar Pocket. *Journal of Biological Chemistry* 274, 2758–2765.

486 Stathatos, G. G., Merriner, D. J., O'Connor, A. E., Zenker, J., Dunleavy, J. E. and O'Bryan, M. K.
487 (2024). Epsilon tubulin is an essential determinant of microtubule-based structures in
488 male germ cells. *EMBO Rep* 25, 2722–2742.

489 Stierhof, Y. D., Ilg, T., Russell, D. G., Hohenberg, H. and Overath, P. (1994). Characterization of
490 polymer release from the flagellar pocket of Leishmania mexicana promastigotes.
491 *The Journal of cell biology* 125, 321–331.

492 Sunter, J. and Gull, K. (2017). Shape, form, function and *Leishmania* pathogenicity: from
493 textbook descriptions to biological understanding. *Open Biol.* 7, 170165.

494 Sunter, J. D., Yanase, R., Wang, Z., Catta-Preta, C. M. C., Moreira-Leite, F., Myskova, J.,
495 Pruzinova, K., Volf, P., Mottram, J. C. and Gull, K. (2019). *Leishmania* flagellum
496 attachment zone is critical for flagellar pocket shape, development in the sand fly,
497 and pathogenicity in the host. *Proc. Natl. Acad. Sci. U.S.A.* 116, 6351–6360.

498 Tran, K. D., Vieira, D. P., Sanchez, M. A., Valli, J., Gluenz, E. and Landfear, S. M. (2015).
499 Kharon1 Null Mutants of Leishmania mexicana Are Avirulent in Mice and Exhibit a
500 Cytokinesis Defect within Macrophages. *PLoS ONE* 10, e0134432.

501 Turk, E., Wills, A. A., Kwon, T., Sedzinski, J., Wallingford, J. B. and Stearns, T. (2015). Zeta-
502 Tubulin Is a Member of a Conserved Tubulin Module and Is a Component of the
503 Centriolar Basal Foot in Multiciliated Cells. *Current Biology* 25, 2177–2183.

504 van Breugel, M., Wilcken, R., McLaughlin, S. H., Rutherford, T. J. and Johnson, C. M. (2014).
505 Structure of the SAS-6 cartwheel hub from Leishmania major. *eLife* 3, e01812.

506 Varadi, M., Anyango, S., Deshpande, M., Nair, S., Natassia, C., Yordanova, G., Yuan, D., Stroe,
507 O., Wood, G., Laydon, A., et al. (2022). AlphaFold Protein Structure Database:
508 massively expanding the structural coverage of protein-sequence space with high-
509 accuracy models. *Nucleic Acids Research* 50, D439–D444.

510 Vats, K., Tandon, R., Roshanara, Beg, Mirza. A., Corrales, R. M., Yagoubat, A., Reyaz, E., Wani,
511 Tasaduq. H., Baig, Mirza. S., Chaudhury, A., et al. (2023). Interaction of novel proteins,
512 centrin4 and protein of centriole in Leishmania parasite and their effects on the
513 parasite growth. *Biochimica et Biophysica Acta (BBA) - Molecular Cell Research* 1870,
514 119416.

515 Vaughan, S., Attwood, T., Navarro, M., Scott, V., McKean, P. and Gull, K. (2000). New tubulins
516 in protozoal parasites. *Current Biology* 10, R258–R259.

517 Wang, J. T., Kong, D., Hoerner, C. R., Loncarek, J. and Stearns, T. (2017). Centriole triplet
518 microtubules are required for stable centriole formation and inheritance in human
519 cells. *eLife* 6, e29061.

520 Wheeler, R. J., Gluenz, E. and Gull, K. (2015). Basal body multipotency and axonemal
521 remodelling are two pathways to a 9+0 flagellum. *Nat Commun* 6, 8964.

522 Wirth, D. F. and Slater, C. (1983). Isolation and characterization of an α-tubulin gene from
523 *Leishmania enriettii*. *Molecular and Biochemical Parasitology* 9, 83–92.

524 Wu, J. and Akhmanova, A. (2017). Microtubule-Organizing Centers. *Annu Rev Cell Dev Biol*
525 33, 51–75.

526

527 **Figure Legends**

528 **Fig 1. Sequence homology of Lmε-tubulin with its counterparts in other organisms.**
529 Sequence alignment of Lmε-tubulin with epsilon-tubulins from *Homo sapiens* (Hs-ε-tubulin)
530 *Chlamydomonas reinhardtii* (Cr-ε-tubulin) *Paramecium tetraurelia* (Pt-ε-tubulin)
531 *Tetrahymena thermophila* (Tt-ε-tubulin). Yellow-shaded region indicates the GTPase domain
532 and green-shaded region indicates the C-terminal domain as predicted by InterPro analysis.
533 Residues marked by black boxes indicate lethal or slow-growing mutations in *Tetrahymena*
534 *thermophila.* Black triangles indicate GTP-binding residues of tubulins as predicted by InterPro
535 analysis.

536 **Fig 2. Genomic PCR and RT-PCR analysis of Lmε-tubulin** [A] Schematic diagram of the
537 chromosome 21 locus containing *Lmε-tubulin* and the adjacent genes. Binding sites of the Lmε-
538 tubulin-specific primers (P1/P2) are shown. [B] Agarose gel image showing PCR amplification
539 of 1413 bp *Lmε-tubulin* genomic locus with primer sets P1/P2. [C] Expression of Lmε-tubulin
540 mRNA in *L. major* promastigotes by RT-PCR using P1/P2. The lanes marked as '+RT' and
541 '−RT' represent the reactions with and without RT enzyme, respectively. [D] Workflow for
542 checking of expression of Lmε-tubulin mRNA in *L. major* amastigotes. [E] Expression of Lmε-
543 tubulin mRNA in *L. major* amastigotes by RT-PCR using P1/P2. The lanes marked as '+RT'
544 and '−RT' represent the reactions with and without RT enzyme, respectively. +IMΦ and -IMΦ
545 indicates RNA extracted from infected and uninfected macrophages, respectively.

546 **Fig 3. Localization of mNG-tagged epsilon-tubulin in promastigote and amastigote stage**
547 ***of L. major*.** [A] Cartoon diagram showing wild-type (WT) Lmε-tubulin genomic locus and
548 engineered mNG- Lmε-tubulin genomic locus following CRISPR-Cas9-mediated endogenous
549 tagging. [B] Whole cell lysates from WT, LmCas9:T7Pol and mNG-Lmε-tubulin expressing
550 *L. major* strain was subjected to SDS-PAGE and the protein expression was checked by western
551 blotting using antibody against mNG (upper), and actin (lower) as housekeeping control. An

552 82.8.7 kDa band corresponding to the molecular weight of the fusion protein (31.1 kDa:
553 3XMyc-mNeonGreen, and 51.7 kDa: Lmε-tubulin) was detected. [C] Confocal microscopy
554 of mNG-Lmε-tubulin expressing *L. major* promastigotes. Cells were fixed and mounted in
555 DAPI (blue) containing mounting media to stain the nuclei and the kinetoplast. Green signal
556 represents mNG-ε-tubulin localization. Merged panel represent the combined image of DAPI
557 along with mNG-ε-tubulin. Merged BF represent the fluorescent signal overlay on brightfield
558 image captured simultaneously showing two distinct green signals, one in close association
559 with the kinetoplast DNA and the other at the base of the flagella. The white box represents the
560 area that has been zoomed and represented as magnified panel. The scale bar represents 10μm.
561 The white arrow represents the bright spot of mNG-ε-tubulin near kinetoplast (K) and yellow
562 arrow represent bright spot away from kinetoplast. The nucleus is marked as 'N' [D] J774A.1
563 macrophages were infected with mNG-Lmε-tubulin expressing *L. major* cells. ~ 60 hours post
564 infection cells were fixed, and mounted with DAPI-containing mounting media and imaged in
565 a confocal microscope. Parasite nuclei (N) and kinetoplast (K) and macrophage nucleus (MϕN)
566 were stained with DAPI (blue), mNG-ε-tubulin is represented by the green signal. Merged
567 image represent the combined image of DAPI along with mNG-ε-tubulin. Merged BF represent
568 the fluorescent signal overlay on brightfield image captured simultaneously. The white box
569 represents the area that has been zoomed and represented as magnified panel. The scale bar
570 represents 10 μm. Two bright spots of mNG-ε-tubulin can be seen in the amastigotes too, one
571 closely associated with the kinetoplast (white arrow) and the other distal from the kinetoplast
572 (yellow arrow).

573 **Fig 4. Nocodazole sensitivity assay for tubulins.** [A] mNG-ε-tubulin distribution in the
574 untreated (left panel) and 1 μM nocodazole treated (right panel) *L. major* promastigotes
575 expressing mNG-ε-tubulin. Nucleus and kinetoplast are stained with DAPI (blue). Green signal
576 represents mNG-ε-tubulin localization. [B] Bar graph showing percentage of cells where ε-

577 tubulin distribution remained unaltered after mock (only DMSO) or 1 μM nocodazole
578 treatment. [C] mNG-α-tubulin distribution in the untreated (left panel) and 1 μM nocodazole
579 treated (right panel) *L. major* promastigotes expressing mNG-α-tubulin. Nucleus and
580 kinetoplast are stained with DAPI (blue). Green signal represents mNG-α-tubulin
581 localization [D] Bar graph showing percentage of cells where alpha-tubulin distribution
582 remained unaltered after mock (only DMSO) or 1 μM Nocodazole treatment. At least 120 cells
583 were quantified from three independent experiments and presented as ±SD. n.s., non-
584 significant; **$p \leq 0.01$.

Figure 1

```
Lmε-tubulin     MPREIVTVQVGQCGNQLGQRWFDVMLQEHKAYPHFPE---ARDAVFL----------- 44
Hsε-Tubulin     -MTQSVVVQVGQCGNQIGCCFWDLALREHAAVNQKGIYDEAISSFFRNVDTRVVGDGGS- 58
Crε-tubulin     MPRELVTIQVGQCGNQVGCRFWELALREHAAYNTKGVYDEALSSFFRNVDTRVEPPRNLP 60
Ptε-tubulin     MPRELIFVQVGQCGNQIGMRFWDLALKEHAKAKQSLLYDESLSSFFRNVN--SKN-QELK 57
Ttε-tubulin     -MRELITIQVGQCGNQIGAKFWELAIKEHSKYNKSSVYDDALSSFFRNIDKSSKG-HELK 58
                   : : :********:*  :::: ::**           : .:.*

Lmε-tubulin     --EAMNHPGRLKARCVAVDMEQGVLHAMLRGPLKDIFDANFFVSDVSGAGNNWAVGHMEY 102
Hsε-Tubulin     --ISKGKICSLKARAVLIDMEEGVVNEILQGPLRDVFDTKQLITDISGSGNNWAVGHKVF 116
Crε-tubulin     VGEGRGAIRTLKARSVIVDMECGVINEMLKGPLGEVLDTRQLVSDVSGAGNNWAHGHHEY 120
Ptε-tubulin     IG---DPIQNLKARALIVDMEEGVINQIMKSPLGELFEERQCINDVSGAGNNWAHGFYHY 114
Ttε-tubulin     VG---SEIINLKARSIIVDMEEGVTNQLLKSDIGDLFDQRQFINDVSGAGNNWAHGHFFY 115
                     .    ****.: :*** ** : :::. : :::: .  :.*:**:***** *.  :

Lmε-tubulin     GDRYIDAIAESVRNQVEQCNCIQSFFLMHSLSGGTGSGLGTRVLGMLEDEFPHVFRICPV 162
Hsε-Tubulin     GSLYQDQILEKFRKSAEHCDCLQCFFIIHSMGGGTGSGLGTFLLKVLEDEFPEVYRFVTS 176
Crε-tubulin     GPRYHDAILDKIRLTAEDCDSLQSFMVLHSLGGGTGSGVGTYIVRMLADEFPGVFRFTGS 180
Ptε-tubulin     GNQYEKHIEERLRKTVEQCDSLQCFFMTHSIGGGTGSGLGSRIVGLLEDNYPEVFRFTAS 174
Ttε-tubulin     GNKYRDNMSERIRKAVEQCDSLQCFFLMHSLGGGTGSGLGTFLLSLIEDEYPDVYRFTAS 175
                *  * . : : .*  .*.*:.:*.*:: **:.******:*: :: :: *::* *:*:

Lmε-tubulin     VMPSEVDDVVTAPYNSCFSLKELIEHADCVLPLDNDALARMADRALSSRPQGRGVMAS-- 220
Hsε-Tubulin     IYPSGEDDVITSPYNSILAMKELNEHADCVLPIDNQSLFDIISKIDLMVNSGKLGTTV-- 234
Crε-tubulin     VFPSEDDDVVTSPYNAMLALGQLVEHADCVLPIENQALIDIVNRTEAARDRAAAADAA-- 238
Ptε-tubulin     VFPSGDDDVVTSPYNSLFSLYELAKHADCVFPIDNQALINIVDQIDKPNKARLVKENAHE 234
Ttε-tubulin     VFPQKDDDVITSPYNSFFSLYELAKHADCVFPIDNQALMNICYQIDNPNKVKLAKDNINV 235
                : *.  ***:*:***: ::: :* :*****:*::*::*  :  :

Lmε-tubulin     -S-------VPQPQAFSAAKPTDTKGLPYDSMNGLVAQLLSNLTCAMRFPGPLNMDINEI 272
Hsε-Tubulin     ----KPKSL----VTSSSGALKKQHKKPFDAMNNIVANLLLNLTSSARFEGSLNMDLNEI 286
Crε-tubulin     ------------ASAVSGLKGSGGGSKPFDSMNGVAASLLLHLTASVRFEGPLNVDLNDI 286
Ptε-tubulin     G---------SVGIKITQFGEEEKRQKPFDKMNSLIAHLLSHITCSMRFEGALNVDLNEI 285
Ttε-tubulin     SKEEEIKIMMNKGSKITQAGTEEKKEKPFDKMNNIIAHLLSNITCSMRFEGVLNVDLNEI 295
                              :           *:* **.: * ** ::*.: ** * **:*:*:*

Lmε-tubulin     TTNLVPFPRLHFLTAAIAPLSVSSK---------HAAVGPRTVDAMITACLDPGHQFVDV 323
Hsε-Tubulin     SMNLVPFPQLHYLVSSLTPLYTLT----------DVNIPPRRLDQMFSDAFSKDHQLLRA 336
Crε-tubulin     TMNLVPYPRMHFLLSSMSPLQPPPKDKDVGRAAAALALQPRTLDQVFGDVFSREHQLIRA 346
Ptε-tubulin     TMNLVPYPDLHFLISSMAPLYSLL----------DSKLQPRRLDQMFNDIYHPDFQMITG 335
Ttε-tubulin     TMNLVPYPDLHFLISSIAPLYSLS----------DSNLQPRRLDQMFKDCYHPDYQLVSV 345
                : ****:* :*:* ::::**                 : ** :* ::       .*::

Lmε-tubulin     RHGQGSAVTREAGKTLATALIARGPQTTVGDLTRGVGRLREQMEMPYWNEDGFKTALCGV 383
Hsε-Tubulin     DP--------KHSLYLACALMVRGNV-QISDLRRNIERLKPSLQFVSWNQEGWKTSLCSV 387
Crε-tubulin     DP--------RAATYLACGLIARGPTATMADINRNVARLRPQLKMVHWNSEGFKLGICST 398
Ptε-tubulin     QP--------SLHKYLAVGLLVRGDV-AFSDVNRNIKKLKDQLKMIYWNQEGFKYGICNQ 386
Ttε-tubulin     NP--------FQNKYLAVGLMVRGSV-PFSDVNRNIKKLRSELNMIYWNQEGFKYGICNT 396
                             ** .*:.**    ..*: *.: :*: .:::  **.:*:* .:*.

Lmε-tubulin     SPLGHKDSMLLLANNCSIRGKVESMLSKYERLYSVRSHVHHYDQY--LSDAYFVHTVETL 441
Hsε-Tubulin     PPVGHSHSLLALANNTCVKPTFMELKERFMRLYKKKAHLHHYLQVEGMEESCFTEAVSSL 447
Crε-tubulin     PPVGCPFGLLCLANNTAIAHTFTTMRERFDKLYKRRFYTHHYEQY--MDPGGFTSAMEVV 456
Ptε-tubulin     PPIGQQYSMLCLANNTCIKDTFQEMTDRFQKLYKRKVYVHHYKQY--MEQSHFDETLNGI 444
Ttε-tubulin     PPIGQPYSLLCLANNTAIRDQFSTMVERFNKLYKRKVFVHHYTEY--MDAKHFDEALNSI 454
                 *:*   .:* **** .:    .  : .:: :**. : . *** :   :.   *  ::. :

Lmε-tubulin     RTLVDDYAYLDTAAPPKDLPRSMKDLIYY--          470
Hsε-Tubulin     SALIQEYDQLDATKNMPVQ-DLPRLSIAM--          475
Crε-tubulin     GDLTAQYRALEGATQAPPLTRLRPRGLSFLP          487
Ptε-tubulin     QNLMVKYQDLEMAQ-PKKYQRIQPIF-----          469
Ttε-tubulin     TSLISKYEELHKAEEPSSQPRLKPLI-----          480
                  *  .*  *. :
```

Figure 2

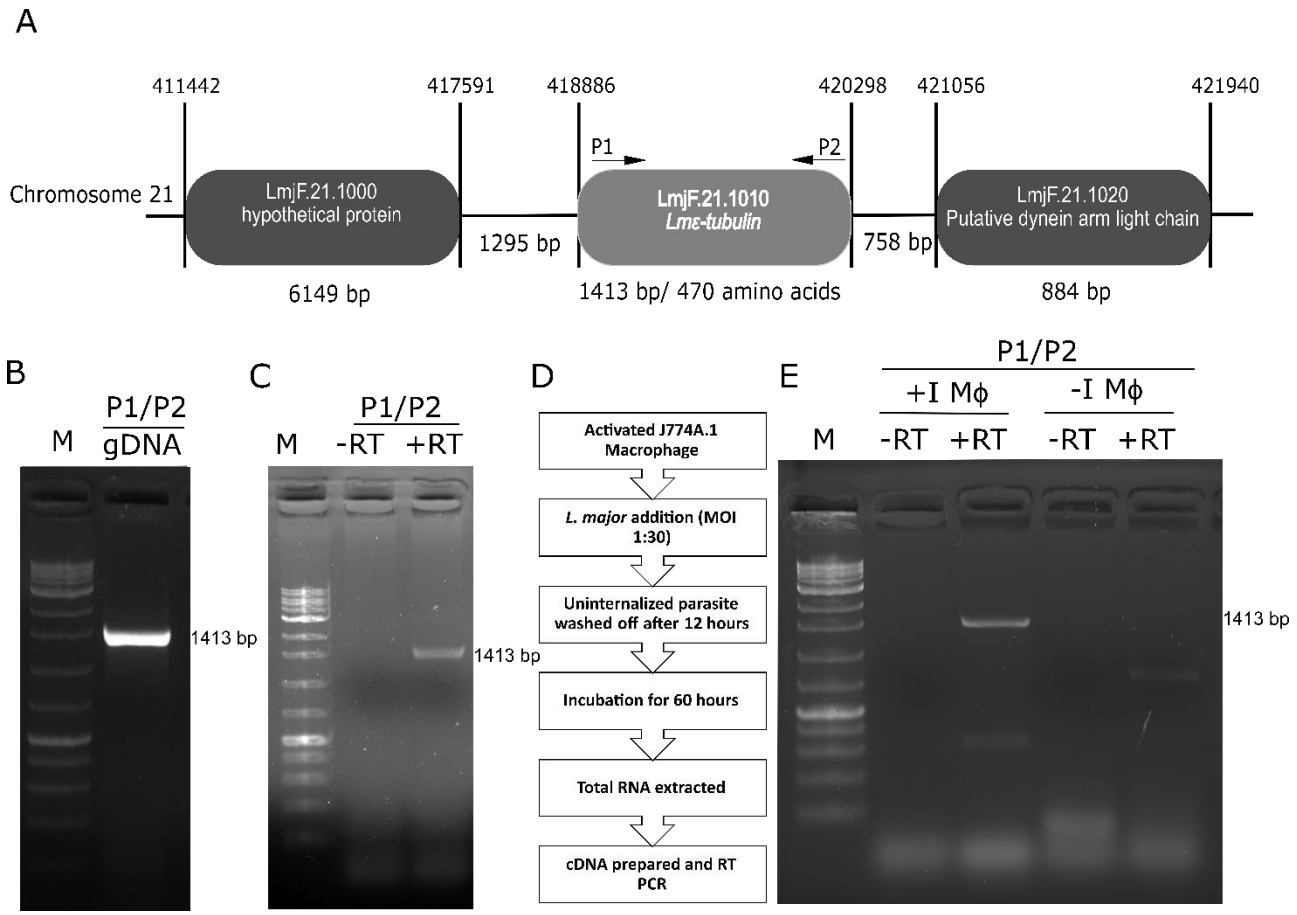
A
411442
417591
418886
420298
421056
421940
Chromosome 21
LmjF.21.1000
hypothetical protein
P1
P2
LmjF.21.1010
Lmε-tubulin
LmjF.21.1020
Putative dynein arm light chain
1295 bp
758 bp
6149 bp
1413 bp/ 470 amino acids
884 bp
B
M
P1/P2
gDNA
1413 bp
C
M
P1/P2
-RT
+RT
1413 bp
D
Activated J774A.1 Macrophage
L. major addition (MOI 1:30)
Uninternalized parasite washed off after 12 hours
Incubation for 60 hours
Total RNA extracted
cDNA prepared and RT PCR
E
P1/P2
+I Mϕ
-I Mϕ
M
-RT
+RT
-RT
+RT
1413 bp

Figure 3

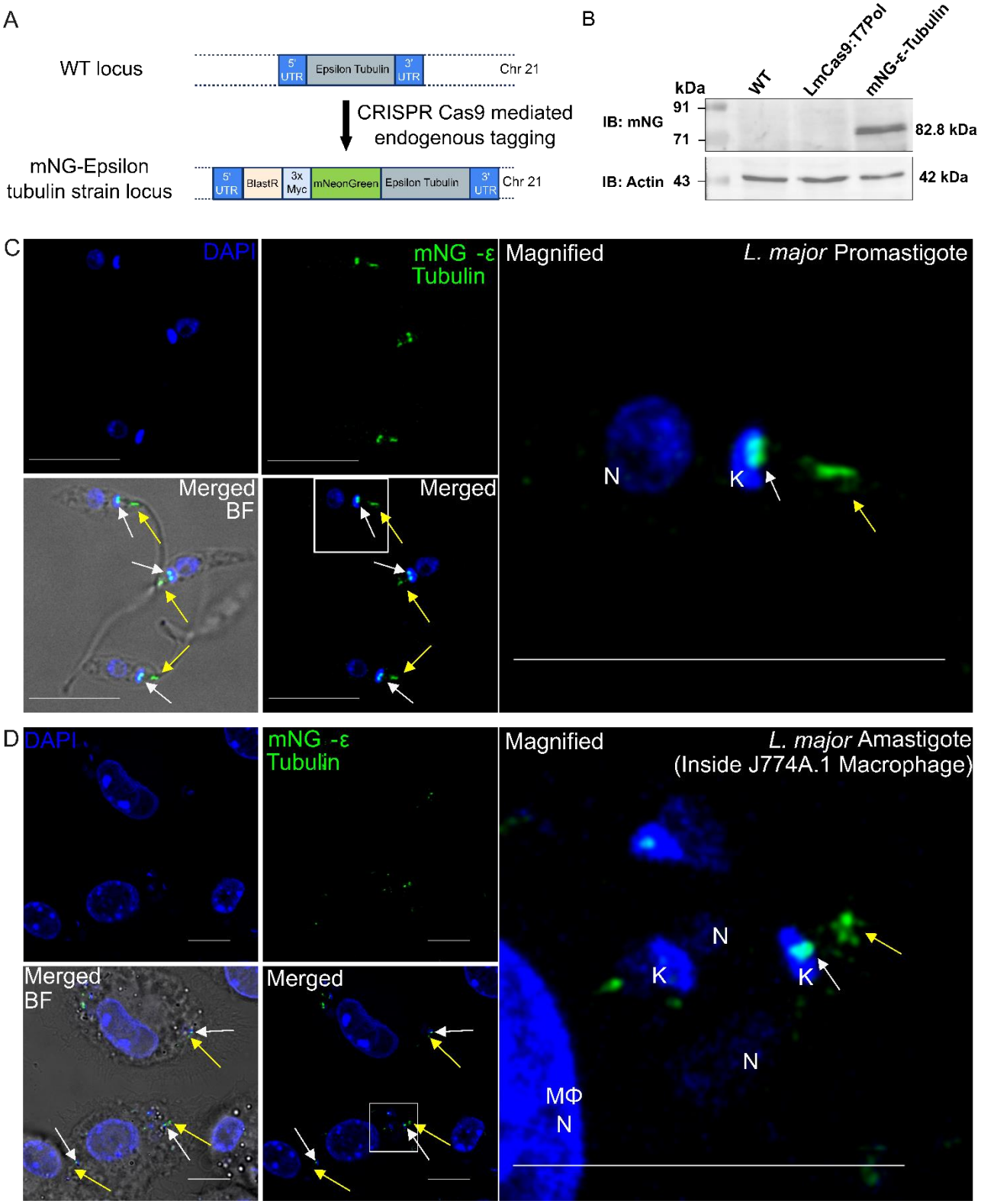
A
WT locus
5' UTR
Epsilon Tubulin
3' UTR
Chr 21
CRISPR Cas9 mediated endogenous tagging
mNG-Epsilon tubulin strain locus
5' UTR
BlastR
3x Myc
mNeonGreen
Epsilon Tubulin
3' UTR
Chr 21
B
kDa
WT
LmCas9:T7Pol
mNG-ε-Tubulin
IB: mNG
91
71
82.8 kDa
IB: Actin
43
42 kDa
C
DAPI
mNG -ε Tubulin
Magnified
L. major Promastigote
N
K
Merged BF
Merged
D
DAPI
mNG -ε Tubulin
Magnified
L. major Amastigote (Inside J774A.1 Macrophage)
N
K
K
N
MΦ N
Merged BF
Merged

Figure 4

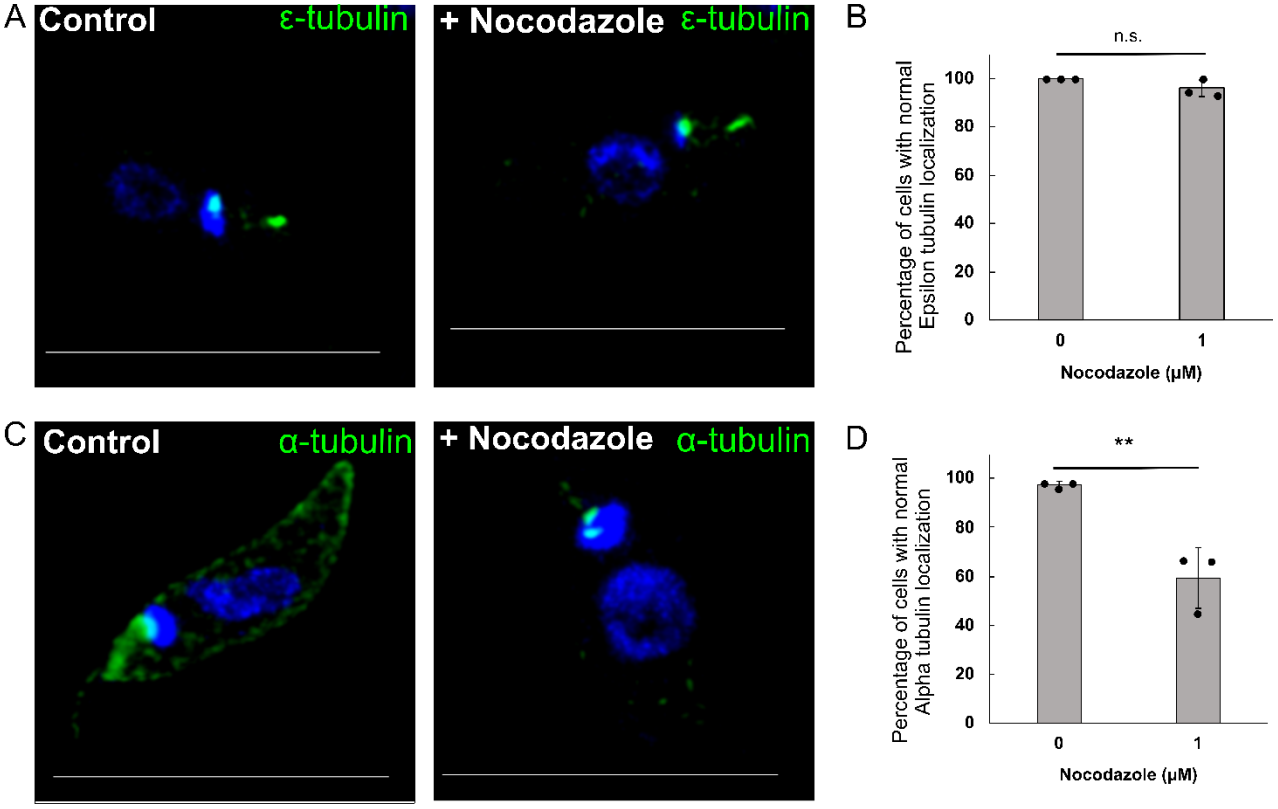
A
Control
ε-tubulin
+ Nocodazole
ε-tubulin
B
n.s.
Percentage of cells with normal Epsilon tubulin localization
100
80
60
40
20
0
0
1
Nocodazole (μM)
C
Control
α-tubulin
+ Nocodazole
α-tubulin
D
**
Percentage of cells with normal Alpha tubulin localization
100
80
60
40
20
0
0
1
Nocodazole (μM)

Supplementary information

A

```
Lmε-tubulin ---VDDVVTAPYNSCFSLKELIEHADCVLPLDNDALARMADRALSSRPQGRGVMASSVPQ     224
Lmγ-tubulin RGGESDVIVQPYNSLLAVKRLTLHADCVVVLDNTALNRIVTDNLHI--------------     222
Lmα-tubulin ---VSTAVVEPYNCVLSTHSLLEHTDVATMLDNEAIYDLTRRSLDI--------------     219
Lmβ-tubulin ---VSDTVVEPYNTTLSVHQLVENSDESMCIDNEALYDICFRTLKL--------------     217
                 . .:. ***  :: : *  ::*    :** *:  :    *

Lmε-tubulin PQAFSAAKPTDTKGLPYDSMNGLVAQLLSNLTCAMRFPGPLNMDINEITTNLVPFPRLHF     284
Lmγ-tubulin ------------ASPTVEQMNGLVSTVMAASTATLRYPGYMNNDLMSMLASLIPTPRCHF     270
Lmα-tubulin ------------ERPSYTNVNRLIGQVVSSLTASLRFDGALNVDLTEFQTNLVPYPRIHF     267
Lmβ-tubulin ------------TTPTFGDLNHLVAAVMSGVTCCLRFPGQLNSDLRKLAVNLVPFPRLHF     265
                                .:* *:. :::  *. :*: * :* *: .: ..*:* ** **

Lmε-tubulin LTAAIAPLSVSSKHAAV--GPRTVDAMITACLDPGHQFVDVRHGQGSAVTREAGKTLATA     342
Lmγ-tubulin VCTGYTPTTLDTSNIQSSVRKTSVHDVMRRLLMPKNMMVSTS--------MKSGCYISLL     322
Lmα-tubulin VLTSYAPVVSAEKA---YHEQLSVADITNSVFEPAGMLTKCD--------PRHGKYMSCC     316
Lmβ-tubulin FMMGFAPLTSRGSQ---QYRGLSVAELTQQMFDAKNMMQAAD--------PRHGRYLTAS     314
            .  . :*     .         :*  :    :     :             . *  ::
```

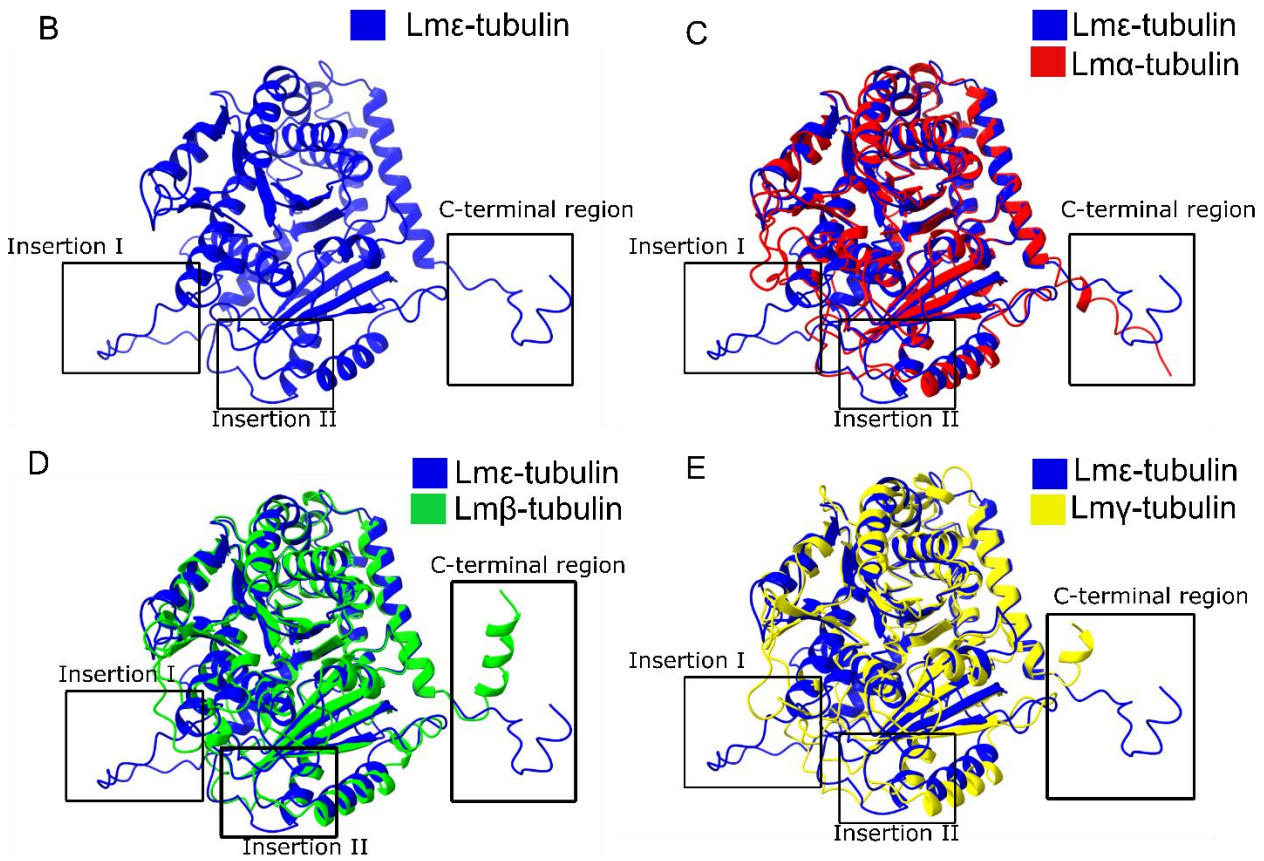

Fig. S1. Sequence and structural alignment of Lmε–tubulin with other conventional tubulins of *L. major*. [A] Lmε-tubulin (168-342) protein sequence was aligned with Lmα-tubulin (177-316), Lmβ-tubulin (175-314) and Lmγ-tubulin (177-322). Although the complete sequence of all the tubulins were aligned, only a portion of the sequence (the exact region mentioned in parenthesis) are represented in the figure. The regions shaded red indicate insertions in Lmε-tubulin that are absent in α, β or γ-tubulins, Insertion I- R211-T236, Insertion II- H325-T332. [B] AlphaFold-predicted structure of Lmε-tubulin, Insertion I, Insertion II and the C-terminal region are marked with boxes. Structural alignments of AlphaFold structure of Lmε-tubulin with that of AlphaFold structures of [C] Lmα-tubulin, [D] Lmβ-tubulin, [E] Lmγ-tubulin. All the structures aligned well with Lmε-tubulin except for three regions, Insertion I, Insertion II and the C-terminal tail.

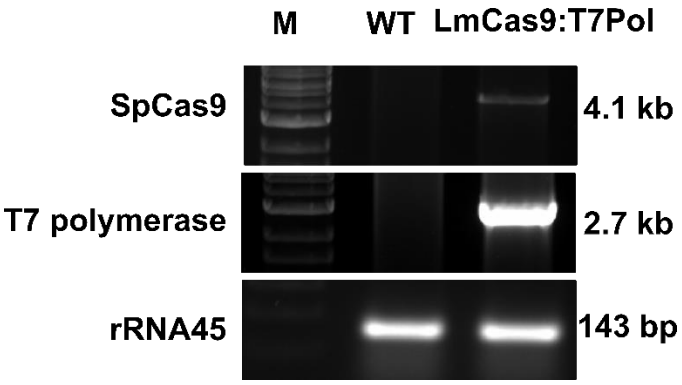

Fig. S2. Verification of LmCas9:T7Pol *L. major* strain. Presence of SpCas9 and T7 polymerase gene in the genome of LmCas9:T7Pol *L. major* cells was checked by PCR. PCR was performed with genomic DNA from wild-type (as negative control) or LmCas9:T7Pol *L. major* cells as templates with specific primers for SpCas9 and T7 Polymerase. 4.1 kb (for SpCas9) and 2.7 kb (for T7 Pol) PCR products in the LmCas9:T7Pol *L. major* cells but not in the WT confirmed proper generation of the strain. PCR for the housekeeping gene rRNA45 was used as loading control.

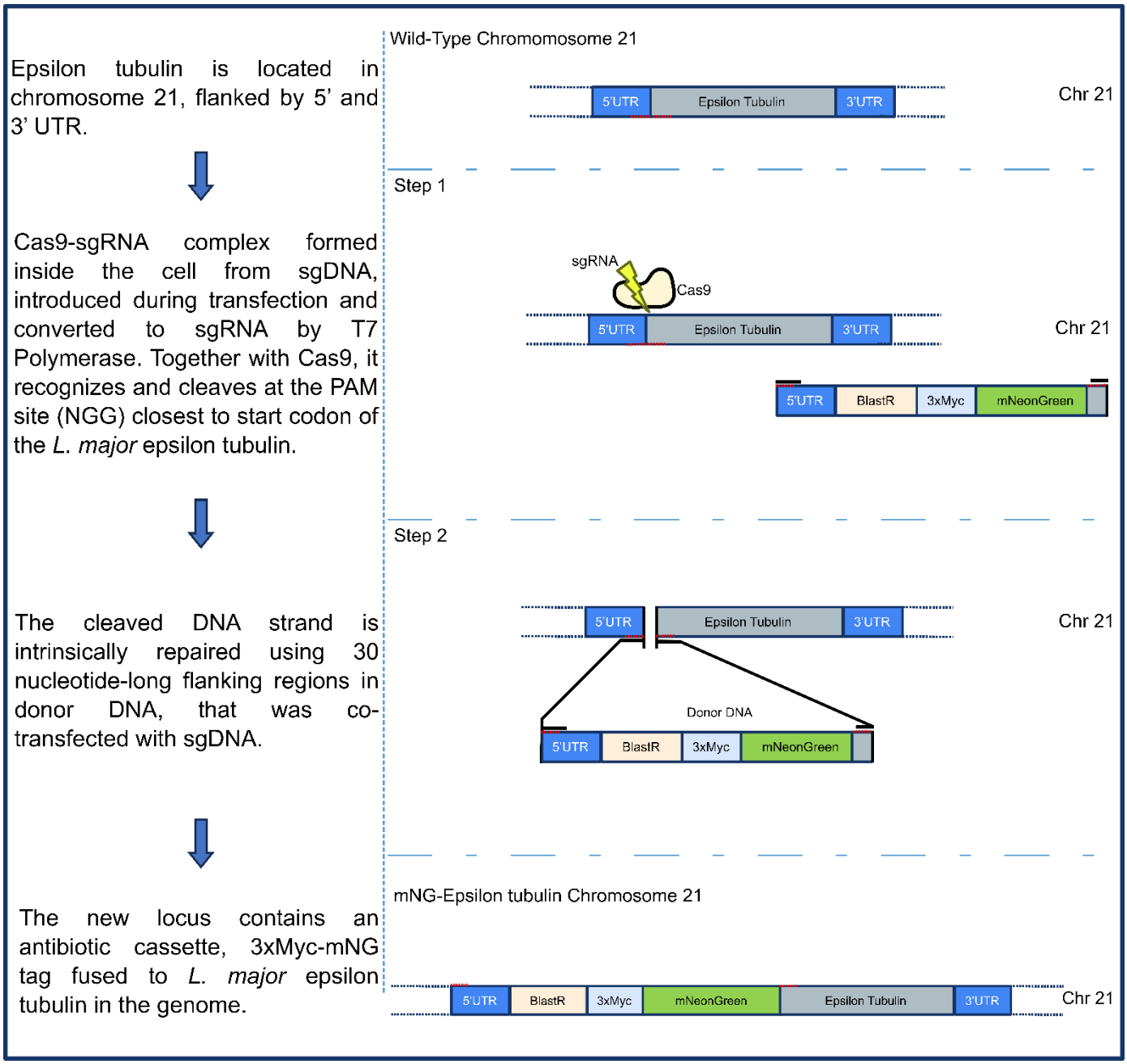

Fig. S3. Scheme for generation of mNG- Lmε-tubulin expressing *L. major* strain. Steps for generation of the N-terminal mNG-tagged-Lmε-tubulin expressing *L. major* strain employing CRISPR-Cas9 endogenous tagging method are described schematically.

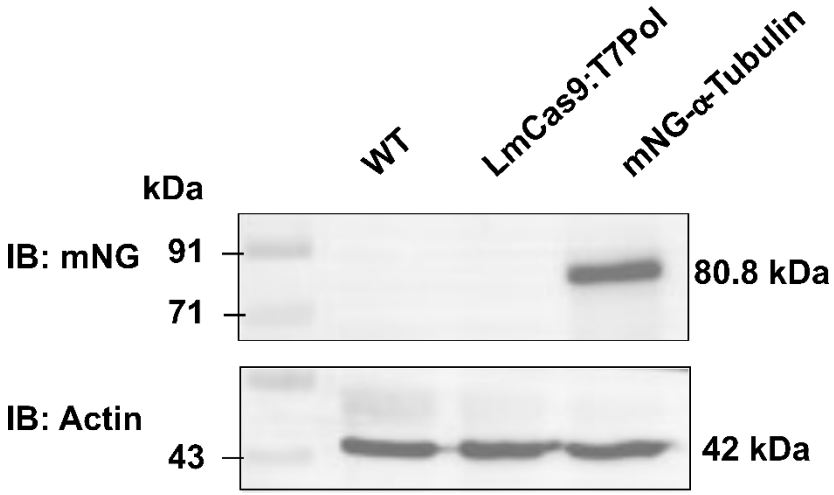

Fig S4. Confirmation of the mNG-Lmα-tubulin expressing *L. major* strain by western blot. Whole cell lysate from wild-type (WT), LmCas9:T7Pol and mNG- Lmα-tubulin expressing *L. major* strain was subjected to SDS-PAGE and the protein expression was checked by western blotting using antibody against mNG (upper), and actin (lower) as housekeeping control. A 80.8 kDa band corresponding to the molecular weight of the fusion protein (31.1 kDa: 3XMyc-mNeonGreen, and 49.7 kDa: Lmα-tubulin) was detected.

Table S1. Percentage identity and similarity of Lmε-tubulin with other organisms

Genus	Species	Percentage identity with *L. major* (%)*	Percentage similarity with *L. major* (%)*
Tetrahymena	*T. thermophila*	40.97	59.43
Chlamydomonas	*C. reinhardtii*	43.83	60.08
Homo	*H. sapiens*	41.37	59.04
Paramecium	*P. tetraurelia*	41.65	61.31
Leishmania	*L. donovani*	98.72	99.15
	L. infantum	98.72	99.15
	L. mexicana	97.23	98.51
	L. braziliensis	91.06	95.96
Trypanosoma	*T. brucei*	68.24	80.12
	T. cruzi	66.80	82.35

***Percentage identity and similarity calculated using NCBI blast**

Table S2. Oligonucleotides used in this paper

Oligo	Primer Sequence (5'-3')	Purpose
G00	AAAAGCACCGACTCGGTGCCACTTTTTCAAGTTGATAACGGACTAGCCTTATTTTAACTTGCTATTTCTAGCTCTAAAAC	Reverse primer for preparation of sgDNA
P1	ATGCCCCCGCGAAATCGTG	Epsilon tubulin forward primer
P2	TTAGTAGTAGATGAGATCCTTCATGCTGCG	Epsilon tubulin reverse primer
P3	GACAAGAAGTACAGCATCGGCCTG	Full-length primer for verification of SpCas9 presence in the genome
P4	GTCGCCTCCCAGCTGAGA	
P5	ATGGAGACGATTAACATCGCTAAGAAC	Full-length primer for verification of T7 pol presence in the genome
P6	CTACGCGAACGCGAAGTC	
P7	CCTACCATGCCGTGTCCTTCTA	rRNA45 primer (used as housekeeping gene)
P8	AACGACCCCTGCAGCAATAC	
P9	TCCACCTTGCCGTGCGCGTGCGTGTGGCCAGTATAATGCAGACCTGCTGC	Upstream forward primer for epsilon tubulin
P10	GACCTGCACCGTCACGATTTCGCGGGGCATACTACCCGATCCTGATCCAG	Upstream reverse primer for epsilon tubulin
P11	GAAATTAATACGACTCACTATAGGGGTGGGACCTTGAGCAGCGCGTTTTAGAGCTAGAAATAGC	Forward primer for preparation of sgDNA against 5' of epsilon tubulin gene
P12	CTCGTTCTTCGAACAAACACCTTTAAACCGGTATAATGCAGACCTGCTGC	Upstream forward primer for alpha tubulin
P13	GCCGATGTGGATGCAGATAGCCTCACGCATACTACCCGATCCTGATCCAG	Upstream reverse primer for alpha tubulin
P14	GAAATTAATACGACTCACTATAGGAAGAAAGAGGGGTTGGAAGGGTTTTAGAGCTAGAAATAGC	Forward primer for preparation of sgDNA against 5' of alpha tubulin gene

Table S3. Antibodies used in this study

Antibody	Host	Source	Catalogue Number	Dilution
mNeonGreen Tag Antibody	Rabbit	Cell Signaling Technology	53061S	WB- 1:1000
Anti-Ld Actin	Rabbit	Gifted by Dr. Amogh Sahasrabuddhe (CSIR-CDRI)	-	WB- 1:20000
Goat Anti-Rabbit I_gG-Peroxidase	Goat	Sigma Aldrich	A9169	WB- 1:4000